Oceanographic habitat and the coral microbiomes of urban-impacted reefs

Stephanie M Rosales [1, 2], **Christopher Sinigalliano** [2], **Maribeth Gidley** [1, 2], **Paul R Jones** [1, 2], **Lewis J Gramer** [Corresp. 1, 2]

[1] Cooperative Institute for Marine and Atmospheric Studies, University of Miami, Miami, FL, United States

[2] Atlantic Oceanographic and Meteorological Laboratory, National Oceanographic and Atmospheric Administration, Miami, FL, United States

Corresponding Author: Lewis J Gramer
Email address: lew.gramer@noaa.gov

Coral reefs are in decline worldwide. In response to this habitat loss, there are efforts to grow, outplant, and restore corals in many regions. The physical oceanographic habitat of corals – such as sea temperature, waves, ocean currents, and available light – is spatially heterogeneous. We therefore hypothesize that outplant location may affect microbiomes, and ultimately, coral health and restoration success. We evaluated the influence of the physical oceanographic habitat on microbes in wild *Porites astreoides* and *Siderastrea siderea*. Tissue samples were collected at four Florida reefs in March, June, and September of 2015. We estimated oceanographic conditions from moored instruments, diver observations, remote sensing data, and numerical models. We analyzed microbiomes using amplicon 16S rRNA high-throughput sequencing data. We found microbial alpha-diversity negatively correlated with *in situ* sea temperature (which represented both the annual cycle and upwelling), as well as modeled alongshore currents, *in situ* sea-level, and modeled tide. Microbial beta-diversity correlated positively with significant wave height and alongshore currents from models, remotely-sensed relative turbidity, and *in situ* temperature. We found that archaea from the order Marine Group II decrease with increases in significant wave height, suggesting that this taxon may be influenced by waves. Also, during times of high wave activity, the relative abundance of bacteria from the order *Flavobacteriales* increases, which may be due to resuspension and cross-shelf transport of sediments. We also found that bacteria from the order SAR86 increase in relative abundance with increased temperature, which suggests that this taxon may play a role in the coral microbiome during periods of higher temperature. Overall, we find that physical oceanographic variability correlates with the structure of these coral microbiomes in ways that could be significant to coral health.

1 **Oceanographic habitat and the coral microbiomes of urban-impacted reefs**

3 Authors: Stephanie M. Rosales [1,2], Christopher Sinigalliano [1], Maribeth Gidley [1,2], Paul R. Jones
4 [1,2], Lewis J. Gramer [*,1,2]
5 Affiliations:
    1. Atlantic Oceanographic and Meteorological Laboratory, National Oceanographic
6
7   and Atmospheric Administration, Miami, Florida, USA
8   2. Cooperative Institute for Marine and Atmospheric Studies, University of Miami,
9   Miami, Florida, USA
10 * Correspondence Author:
11 Lew Gramer[1,2]
12 lew.gramer@gmail.com, +1-305-772-7933

14 Keywords: turbidity, waves, currents, temperature, bacteria, archaea

Abstract

16 Coral reefs are in decline worldwide. In response to this habitat loss, there are efforts to grow,
17 outplant, and restore corals in many regions. The physical oceanographic habitat of corals – such
18 as sea temperature, waves, ocean currents, and available light – is spatially heterogeneous. We
19 therefore hypothesize that outplant location may affect microbiomes, and ultimately, coral health
20 and restoration success. We evaluated the influence of the physical oceanographic habitat on
21 microbes in wild *Porites astreoides* and *Siderastrea siderea*. Tissue samples were collected at
22 four Florida reefs in March, June, and September of 2015. We estimated oceanographic
23 conditions from moored instruments, diver observations, remote sensing data, and numerical
24 models. We analyzed microbiomes using amplicon 16S rRNA high-throughput sequencing data.
25 We found microbial alpha-diversity negatively correlated with *in situ* sea temperature (which
26 represented both the annual cycle and upwelling), as well as modeled alongshore currents, *in situ*
27 sea-level, and modeled tide. Microbial beta-diversity correlated positively with significant wave
28 height and alongshore currents from models, remotely-sensed relative turbidity, and *in situ*
29 temperature. We found that archaea from the order Marine Group II decrease with increases in
30 significant wave height, suggesting that this taxon may be influenced by waves. Also, during
31 times of high wave activity, the relative abundance of bacteria from the order *Flavobacteriales*
32 increases, which may be due to resuspension and cross-shelf transport of sediments. We also
33 found that bacteria from the order SAR86 increase in relative abundance with increased
34 temperature, which suggests that this taxon may play a role in the coral microbiome during
35 periods of higher temperature. Overall, we find that physical oceanographic variability correlates
36 with the structure of these coral microbiomes in ways that could be significant to coral health.

Background

38 Coral reefs face numerous environmental and biological challenges, especially in a changing
39 climate. Understanding how the physical habitat – such as temperature variability, light, and
40 water flow – interacts with biological factors in corals has important implications for managing
41 these sensitive ecosystems. Environmental factors such as wind and surface ocean waves can

42   contribute to the spatial morphology of coral reefs over time (Gischler et al. 2014). Waves help
43   form organismal and morphometric gradients on reefs (Harborne et al. 2006; Kelly et al. 2014;
44   Kench & Brander 2006; Porter et al. 2017), driving both coral breakage and intermittent water
45   flow on shallow reefs. Coral health is dependent as well, on geographically fine-scale ocean
46   circulation, which varies inter-annually, seasonally, and over shorter time scales (Feng et al.
47   2016a; Monismith et al. 2018; Rogers et al. 2013; Shedrawi et al. 2017; Sponaugle et al. 2005).
48   For example, coral larval dispersion and settlement rates are affected by hydrodynamic
49   variability, which ultimately impacts gene flow and the genetic diversity of coral reefs (Baums et
50   al. 2006; Serrano et al. 2014; Serrano et al. 2016).
51   Oceanographic processes can also affect the distribution of nutrients across a reef (Zhang
52   et al. 2011). Currents and upwelling can bring nutrients from the ocean to reefs, and also flush
53   water that has been depleted of nutrients. Nutrient uptake by corals is also augmented by
54   increased wave orbital motion and wave-driven circulation (Hearn et al. 2001; Lowe & Falter
55   2015), especially in shallow reefs (Zhang et al. 2011). Additionally, upwelling on coral reefs -
56   the upward, onshore motion of cooler waters from the subsurface ocean (Gramer et al. 2018;
57   Leichter et al. 1996) - can aid in both survival and recovery from a bleaching event (Bayraktarov
58   et al. 2013; Tkachenko & Soong 2017). For instance, in Tayrona National Natural Park in
59   Colombia, corals that underwent bleaching recovered by 97% in areas where seasonal upwelling
60   occurred (Bayraktarov et al. 2013).
61   The health of corals is associated with the structure and composition of their microbial
62   communities. With healthy corals showing microbial patterns distinct from diseased or stressed
63   colonies (Glasl et al. 2016; Kimes et al. 2010; Roder et al. 2014). Coral microbiomes respond to
64   both biotic and abiotic fluctuations. While many studies have examined the effects of
65   temperature on coral microbiomes (Bourne et al. 2008; McDevitt-Irwin et al. 2017; Zaneveld et
66   al. 2016), fewer studies have examined the relationship of coral microbiomes to other physical
67   oceanographic variables, such as water flow (including tides and wave-driven flow) and
68   available light (or turbidity). A recent study evaluated the changes in microbial communities in
69   the coral *Coelastrea aspera* during a 4 d spring tide event in Phuket, Thailand (Sweet et al.
70   2017). It was observed that spring tides induced changes in microbial composition that were
71   likely driven by transient microbial members. Another recent study showed that *Acropora*
72   *muricata* corals exposed to higher rates of water flow in both tank and *in situ* experiments have a
73   more stable microbiome (Lee et al. 2017). Coral reefs with higher impacts from turbidity showed
74   a relative increase in opportunistic bacterial pathogens, and a decrease in symbiotic bacteria
75   (Ziegler et al. 2016). Also, one recent study found that temperature and available light affected
76   prokaryotic communities associated with the tissue of *Pocillopora damicornis*, a common
77   brooding coral in the Indo-Pacific (van Oppen et al. 2018).
78   Studies like those highlighted above, provide evidence that the physical habitat can
79   impact coral microbial community members and suggests that this may affect the health of the
80   host. In 2008, it was estimated that southeast Florida reefs had less than 5% live coral cover,
81   compared to higher values in prior decades (Gilliam 2009). As a result of this ongoing decline
82   (Lirman et al. 2011), there are now efforts to restore and outplant corals in Florida (Lirman &
83   Schopmeyer 2016; Young et al. 2012). Both site selection and host genetics have been shown to
84   be strong indicators for growth in outplanted corals (Drury et al. 2017). Nonetheless, there is still
85   a lack of information in the literature on precisely which physical habitat characteristics can
86   increase the incidence of beneficial coral microbes and ultimately increase rates of coral survival
87   (Glasl et al. 2016).

88   In our study, we aimed to identify the impacts of the physical oceanographic habitat – in
89 particular, turbidity, temperature, waterflow (currents, waves, tides), and bathymetry – on coral
90 microbiomes. We used a bioinformatics approach to evaluate microbial communities using 16S
91 rRNA amplicon high-throughput sequencing on samples collected in March, June, and
92 September of 2015. These samples were collected from the tissue of two stony coral species in
93 the wild, *Porites astreoides* – a brooding coral considered resilient, but currently being affected
94 by disease in Florida, and *Siderastrea siderea* – a reef-building broadcast spawner also being
95 affected by disease (Edmunds 2010; Walton et al. 2018).
96   Corals were collected from four southeast Florida reefs: Barracuda, Oakland Ridge,
97 Emerald, and Pillars (Table 1 and Fig. 1). Physical habitat variables were investigated after
98 sample collections were completed. We used longitude and latitude coordinates and dates that
99 coral tissue was sampled to extract oceanographic habitat data from an operational wave model,
100 a quasi-operational ocean-circulation model, and satellite remote sensing products. In-water
101 measurements of temperature were recorded at the sampling sites. Seafloor moorings near the
102 study region collected data on current profiles, sea temperature, and seafloor pressure.
103   In this paper, we summarize variability in the physical habitat across the three sampling
104 months and the four reefs. We then seek correlations between the physical habitat and coral
105 microbiome data using stepwise linear regression models. Our data show that independent of the
106 physical habitat, coral-host species had a strong correlation with microbial composition. Yet, for
107 both host species, physical oceanographic variables, as well as month of sampling and reef
108 location, were all significant in structuring microbiomes. Our analysis suggests that the physical
109 habitat may contribute to changes in the coral microbial community over both time and space.
110

Methods

Study region

113 The Florida reef tract (FRT) is a coral reef system in the USA, that stretches from the Dry
114 Tortugas (83.0 W, 24.5 N) east and north to the lower edge of the South Atlantic Bight (80.0 W,
115 27.3 N). The northern third of the FRT lies along the southeast Florida shelf, offshore of Miami-
116 Dade, Broward, and two other counties. For this study, four reefs were sampled (Fig. 1):
117 Barracuda and Oakland Ridge reefs in Broward, and Emerald and Pillars reefs in Miami-Dade.
118 Three distinct sites within each reef were selected for replicate coral tissue collections, resulting
119 in a total of 12 sampling sites. These sites are in waters between 6 and 12 m deep, and lie
120 between 1.1 to 5.5 km offshore of mainland Florida.

Sample collection

122 The data for this study were leveraged from previous projects. Details about the sites and
123 collection methods have previously been presented (Sinigalliano et al. 2018; Staley et al. 2017).
124 Briefly, samples for this study were collected during March, June, and September of 2015 (see
125 Table 1). Visually healthy corals were sampled at random from two coral species, *Porites*
126 *astreoides* and *Siderastrea siderea*, with SCUBA and a syringe biopsy method. This entailed
127 loosening the polyps from the calyx by gently scrapping/digging at the polyp tissue before

128   adhering a 5 mL syringe against the coral polyp to create a suction and extract that polyp from
129   the coral head. This was repeated twice per coral head and combined into one sample in the lab.
130   When divers reached the boat, samples were transferred to a 50 mL tube with 45mL of 95%
131   molecular grade ethanol, placed on ice, then preserved at -80°C at the NOAA AOML laboratory.
132   In addition, divers measured sea temperature with a dive-watch (see Physical oceanographic
133   habitat analysis), and both overall and per-species coral cover and coral mean size (Sinigalliano
134   et al. 2018) at each of the reef sites. A total of 24 *P. astreoides* and 31 *S. siderea* samples were
135   collected across four reefs (Barracuda, Oakland Ridge, Emerald, and Pillars) during the three
136   months of sampling (March, June, and September).

DNA extractions and microbiome amplicon sequencing

138   Coral polyps, which included the tissue and remnant mucus, were processed for DNA extraction
139   and sequencing, briefly as follows (Staley et al. 2017): samples were vortexed to resuspend coral
140   tissue, and the entire contents were placed on a 0.2 μm polycarbonate filter under a vacuum.
141   Both the filter and any residual large coral tissue were transferred to a bead beating Lysing
142   Matrix "E" tube. The samples were then homogenized by bead beating with a FastPrep 24
143   instrument (MP, Biomedical) by two separate rounds of bead beating at an impact speed of 6.0
144   m/s for 60 seconds each (for a total of 120 seconds at 6 m/s). Each lysed sample was then
145   purified with the FastDNA SPIN kit for soil DNA Extraction (MP, Biomedical) following the
146   manufacturer's instructions and eluted in 100μL of TE buffer. DNA was amplified using dual
147   index primers, 515F and 806R, that target the variable-4 (V4) region of the 16S rRNA gene.
148   Amplified DNA was sequenced on the MiSeq platform, generating paired-end reads of 300 base
149   pairs (bps).

Bioinformatic analysis

151   Demultiplexed sequences from the 55 samples were retrieved from the National Center for
152   Biotechnology Information (NCBI) Sequence Read Archive (SRA) database (#SRP076111).
153   Once downloaded, the sequence primers were trimmed using the program `cutadapt`. The
154   sequences were analyzed with `qiime2-2018.6` using the DADA2 pipeline for classification
155   of amplicon sequence variants (ASVs), and were run with a max expected error (maxEE) of 2
156   (Callahan et al. 2016). To select sequence trimming positions, the quality score of a random set
157   of sequences were analyzed. Where sequences showed a drop-in quality score (<Phred= 30),
158   those base pair (bp) positions where chosen for trimming. All forward sequences were truncated
159   to the same length of 220 bps and trimmed at the first 8bps. The reserve reads were also
160   truncated to be of the same length at 120 bps, and trimmed at the first 20 bps. The DADA2
161   pipeline was used for ASV selection, dereplication, merging paired-end reads (min overlap
162   =20bps) and removing chimeras (with the "consensus" option). Taxonomy was assigned with the
163   Silva database version132 training set, which was trained on the V4 region by the `fit-`
164   `classifier classify-sklearn` function. Only sequences that were taxonomically
165   identified as Bacteria or Archaea were analyzed. The biome data, ASV table, fasta file,
166   phylogenetic tree, and metadata for this analysis can be found on figshare
167   (DOI:10.6084/m9.figshare.7388672). The specific NCBI accession number for each sequence
168   file is listed under "sampleID" in the metadata file.

Statistical analysis

Microbial alpha-diversity was evaluated with `qiime2-2018.6`, using the Shannon diversity index and species evenness metrics. To asses alpha-diversity, ASV counts were rarefied to (randomly filtered to an equal sequencing depth of) 403 counts, so that all 55 samples could be evaluated. Since 403 is a low number of sequences, the ASV table was also rarefied to 2,055 (N=53). We compared these two methods and since both methods resulted in the same conclusions, a rarefaction of 403 was used in order to include all 55 samples in alpha-diversity analysis. Categorical habitat data (see Table 1) were tested for significant relationships with Shannon diversity index and species evenness using the `alpha-group-significance` function, which applies a pairwise/all-group Kruskal-Wallis test (Gregr & Bodtker 2007). Continuous habitat data (see Table 1) were tested vs. alpha-diversity with a simple linear regression, using the function `lm` on R.3.4.3.

For beta-diversity tests, the data were not rarefied, but instead were filtered by retaining only those taxa that were seen four or more times in at least 10% of the samples. The counts were then transformed into relative abundances. Continuous habitat data were evaluated for pairwise covariance; from each pair with a correlation >80%, one variable was selected for further analysis. Principal coordinate analysis (PCoA) ordination was applied to the relative abundance of ASVs with a weighted UniFrac distance metric (Lozupone & Knight 2005). Discrete variables (i.e., reef site, species, and month) were tested using Analysis of similarities (ANOSIM) and a Permutational multivariate analysis of variance (PERMANOVA) with 999 permutations to identify which groups were different (Clarke & Warwick 1994). The counts matrix was also used to build a model with forward and backward model selection, using the Vegan function `ordistep`, which selects significant variables that best explain the counts data. Prior to inputting habitat variables into `ordistep`, their respective variance-inflation factors (Salmeron et al. 2018) (VIF) were tested; variables with a VIF score >20 were removed from further analysis. The variables selected by the model were then used to construct a canonical or constrained correspondence analysis (CCA) (Henriques et al. 2006). These statistical analyses were conducted with the packages Vegan 2.4.6 and phyloseq 1.22.3.

To further evaluate patterns seen in the beta-diversity results, we used a classification method to evaluate which microbial taxa were important to the physical habitat variables that were found to be significant using ordistep (above). The classification method used on each of the significant physical habitat variables was the `sample-classifier regress-samples` function from qiime2. This function performs random forest (a supervised machine learning algorithm) and was used with parameters --p-parameter-tuning, --p-estimator RandomForestRegressor (RFR), and --p-n-estimators 500. The model outputs importance values and the highest importance values have the greatest prediction power. Thus, the five taxa with the highest importance values from each random forest test were selected for simple linear regression analysis vs. the corresponding physical habitat variable. Only the taxa with a significant correlation ($p < 0.05$) and a coefficient of determination $R^2 > 0.2$ were plotted. The code for the statistical analysis for the microbial data and the corresponding figures are found on figshare (DOI:10.6084/m9.figshare.7925495).

Physical oceanographic habitat analysis

210

211   The minimum near-bottom sea temperatures were collected by divers (see **Sample collection**).
212   Replicates for each measurement are listed in Table 1. Seafloor depths (bathymetry) were
213   derived from NOAA's 10 m horizontal-resolution port-bathymetry project (Carignan et al.
214   2015). From bathymetry, we estimated local seafloor depth ([m]), seafloor slope (rise/run),
215   isobath orientation (alongshore direction, deg. True), and distance from each sampling site to the
216   nearest major inlet running through the Intracoastal Waterway (Fig. 1 and Table 1).
217   Satellite multispectral ocean-color was used to produce a proxy for in-water turbidity, a
218   product called relative turbidity or color index (CI). Since 2000, the MODerate-resolution
219   Imaging Spectrophotometer (MODIS) instruments aboard the polar-orbiting Aqua and Terra
220   satellites have produced multispectral ocean color data at 250 m horizontal resolution. CI
221   datasets were produced from these data, using an algorithm developed by the University of South
222   Florida's Optical Oceanography Laboratory (Barnes et al. 2015).
223   The CI product is subject to bias in shallow waters where the seafloor may be visible
224   from space. In this study, CI values were normalized using the median and 7th and 93rd
225   percentiles for 15 years of CI data (2000-2015) from each pixel. Percentile values were used
226   because CI for coastal pixels is often not normally distributed (Gramer & Hendee 2018). On days
227   when clouds obscured a pixel during one or both daytime satellite overpasses, no CI value was
228   available for that site. Therefore, for the purposes of this study, we used a 14 d arithmetic mean
229   of CI values centered on each sample date, resulting in relative turbidity time series with no gaps
230   (Fig. 2A-C). Finally, time series for satellite CI were validated by linear regression vs. in-water
231   turbidity measurements (NTU) done with boat-based casts using a factory-calibrated
232   nephelometer throughout the sampling period (2013-2015) (Supplementary Fig. S1; Staley et al.
233   2017).
234   Ocean currents were extracted as daily snapshots from the Gulf of Mexico HYbrid-
235   Coordinate Ocean Model (GoM HYCOM; Gierach et al. 2009) at the vertical layer closest to the
236   surface. Northward and eastward vector-components were bilinearly interpolated from native
237   model resolution (1/25th degree) to individual sampling location. Current vectors were then
238   rotated so that positive cross-shore currents were directed perpendicular to the local isobath (i.e.,
239   "offshore") at each site. Daily snapshots of currents from GoM HYCOM alias the diurnal and
240   semidiurnal tidal cycles, showing the distinct signature of the 27.55 d M_m tidal constituent.
241   Furthermore, although we expect GoM HYCOM to provide useful statistics for the amplitude of
242   lower-frequency (multi-day) current variability, the model may not always correctly model the
243   phase of that variability (Gramer 2013). Thus, centered moving 14 d averages of each current
244   component (cross-shore and alongshore) were analyzed (Fig. 2D-F).
245   To estimate surface wave action, we used significant wave height from NOAA's
246   WaveWatch III multi-mesh grid operational model for the western Atlantic, with 4 nautical-mile
247   nominal resolution (Lee et al. 2009; Tolman 2014). A wave attenuation algorithm was applied to
248   wave height, bilinearly interpolated to the horizontal resolution of the bathymetry (10 m)
249   (Supplementary Fig. S2; Gramer & Hendee 2018). This algorithm linearly reduces significant
250   wave height at bottom-depths between 0-20 m, resulting in high-resolution wave fields that reach
251   all the way inshore, with zero wave-height at the beach (Supplementary Fig. S3).
252   Ocean model outputs and diver-watch sea temperatures were validated using *in situ*
253   hourly observations from acoustic Doppler current profilers (ADCP) (Supplementary Fig. S4).
254   These ADCPs were moored at two sites, one at 7 and one at 26 m depth, 6 km north of

255 Barracuda Reef (Sinigalliano et al. 2018). They measured near-bottom sea temperatures
256 (nominal accuracy 0.01 K) and three-dimensional ocean current profiles (bin sizes 0.5 m at 7 m
257 depth and 1 m at 26 m, nominal accuracy 10^{-4} m s^{-1}) every 20 min throughout all three sampling
258 periods of March, June, and September of 2015.
259   Tide heights for each site were modeled using the TPXO 7.2 global tide solution
260 (Stammer et al. 2014). Hourly *in situ* measurements of near-bottom sea-pressure from the FACE
261 mooring at 7 m depth were also used with mean depth removed ("sea-level anomaly"), both to
262 validate model tide-stage predictions and to consider the additional effects of setup from wind,
263 waves, and larger-scale sea-level variation offshore. The time of day of collection was not logged
264 for the tissue samples analyzed in this study, nor can the TPXO 7.2 global solution model fine-
265 scale variability in tide heights and currents on the topographically complex southeast Florida
266 shelf (~1 km, diurnal or faster). For these reasons, a 14 d centered average of both the modeled
267 tide height and the sea-level anomaly (Supplementary Fig. S5) were analyzed in the present
268 study. The Ecoforecasts toolkit, a set of MATLAB functions developed by Gramer as a part of
269 NOAA CHAMP, was used to produce some time series analyses and maps presented here. Due
270 to the prevalence of non-Gaussian distributions in habitat data (Supplementary Fig. S6), results
271 for habitat variables are cited as median ± half of interquartile range values. Elsewhere, e.g., for
272 relative abundances, mean and standard deviation are reported. The code used to generate
273 physical ocean habitat variables and the corresponding figures are found on figshare (DOI:
274 10.6084/m9.figshare.7925546).
275

Results

277 ## The physical oceanographic habitat of four southeast Florida coral reefs in
278 2015

279
280   To extract all other physical habitat variables for each of the four reefs, we used longitude
281 and latitude coordinates from each of the 12 sample-collection sites (three sites per reef, Fig. 1)
282 together with the dates of sampling, as described in the **Methods**. March was a period of
283 geographic patchiness in CI (Fig. 2A). However, patchiness was largely confined during March
284 sampling dates to waters away from the sampling sites. On the other hand, both June and
285 September (Fig. 2B-C) showed less intense regional patchiness, but patches of higher relative
286 turbidity did reach some of the sites during sampling. Satellite relative turbidity (CI) showed a
287 complex seasonal pattern than the other variables considered (Fig. 3C). The highest extreme and
288 the greatest range of values occurred during June sampling (-0.43 to 0.23, median -0.16), with
289 sampling in September scattered over a mainly lower range (-0.50 to -0.08, median -0.23), and
290 that from March clustered within a very narrow range (-0.13 to -0.04, median -0.09). Barracuda
291 was the reef that experienced the greatest positive and negative extremes of normalized CI
292 during the 2015 sampling, with a peak at the three Barracuda sites of between +0.06 and +0.23
293 on the sampling day of June 12th, and lows between -0.30 and -0.50 on September 11th.
294 Interestingly, June was also the month with the highest CI value at Oakland Ridge (0.11), despite
295 lower modeled waves. (Results of regressing satellite CI values vs. in-water turbidity
296 measurements are shown in Supplementary Fig. S1)

297   Alongshore currents from the Gulf of Mexico HYCOM model (Fig. 2D-F and Fig. 3D)
298   showed a relative peak at all sampling sites during June, with weekly medians of +0.30 to +0.65
299   m s^{-1} (positive being a northward current). Further peaks in July and August were followed by a
300   rapid decline during sampling weeks in September, to medians of +0.10 to +0.45, which was also
301   similar to medians during the March sampling. At the time of coral tissue sampling, in *situ* ocean
302   current profilers were deployed near the sampling sites. The midsummer peak could also be seen
303   in these instruments (Fig. 3D, gray and black lines). According to climatology models (Fig. 2E),
304   this summer peak corresponded to a westward meander of the Florida Current; this June meander
305   however affected the southernmost sampling sites, those at Emerald Reef (median +0.60 ± 0.00
306   m s^{-1}), more than at the other three reefs (medians +0.30 to +0.48 ± 0.01 m s^{-1}). Emerald Reef
307   actually experienced higher alongshore currents than the other sites during all three sampling
308   months, although these differences were less extreme in March and September than they were in
309   June.
310   The minimum diver-watch sea temperature was recorded during each tissue-sampling
311   dive (Table 1). For validation, dive-watch temperatures were compared to sea temperatures
312   measured at two moorings (that at 7 and that at 26 m depth). Dive-watch sea temperature
313   followed closely the coincident mooring temperatures at 7 m (Fig. 3A; black line): regressions
314   were significant (p<0.0001, Supplementary Fig. S4), with root mean-squared error (RMSE) 0.28
315   at Barracuda, 0.78 at Oakland Ridge, 0.31 at Pillars, and 0.29 K at Emerald. Regressions vs. the
316   deeper mooring at 26 m were also significant (p < 0.05) with RMSE of 0.8 at Barracuda, 1.0 at
317   Oakland, 0.34 at Pillars, and 0.25 K at Emerald.
318   Like the moorings, dive-watch sea temperature across the four reefs followed a seasonal
319   pattern (Fig. 3A). For March, there was a median 23.2 and interquartile range ±0.4, for June 28.0
320   ±0.2, and for September 29.2 ±0.5 °C. However, temperatures were somewhat cooler than might
321   be expected from historical *in situ* measurements in this region, especially during the warmer
322   months (Gramer et al. 2018). In particular, the mooring at 7 m depth (Fig. 3A) recorded near-
323   bottom temperatures of 24.7 ±0.5 in March, 29.2 ±0.9 in June, and 31.2 ±0.4 °C in September of
324   2015. Similarly, near-surface temperature measurements in 2 m of water at the nearby Virginia
325   Key pier (NOAA National Ocean Service station "VAKF1") showed warmer temperature ranges
326   in June and September of 29.7 ±1.1 and 30.1 ±0.6 °C, respectively (Fig. 3A; red line).
327   Wave heights from the attenuated NOAA model showed a relatively simple seasonal
328   pattern for all sites (Fig. 3B), with the highest waves at all sites during sampling in March (0.25-
329   0.35 m), and intermediate waves during sampling in late September (0.2-0.3 m). Waves in June
330   were generally lower (0.15-0.25 m), due to the absence of storm systems in the nearby Atlantic
331   and Gulf of Mexico, and to generally light local summer winds. The lowest wave estimates,
332   however, were those for samples taken in early September at Oakland Ridge and Barracuda (0.08
333   m); these two reefs were generally the most sheltered (Fig. 1 and Supplementary Fig. S3).
334   Furthermore, these samples were gathered prior to a series of wind events in mid-September, and
335   perhaps more importantly, prior to the development of a major tropical weather system in the
336   Atlantic in late September (Fig. 3B; see **Discussion**).
337   Tide models used for this study do not provide sufficient spatial or phase resolution to
338   estimate diurnal or semidiurnal variability in water heights or tidal currents. However, these
339   models do resolve variability between sites associated with the M_m tidal constituent, which has a
340   27.55 d period. Tide height variations for this constituent were at or near their minimum (-0.008
341   to -0.005 m) during all March sampling dates. In June, sampling was done near the M_m peak
342   (+0.002 m) at all reefs except Oakland Ridge, where samples were gathered near the time of the

343   minimum or ebb M_m (-0.005 m). Similarly, September samples were collected near the ebb at
344   both Oakland Ridge and Barracuda (-0.006 to -0.004 m), and near the peak at Pillars and
345   Emerald Reef (+0.001 m).
346   Unlike with the tide model, sea-level anomaly as estimated from the 7 m mooring shows
347   the effect of sea-level setup from wind and possibly other forcings, in addition to the effect of the
348   barotropic tide (Cushman-Roisin & Beckers 2011). A sea-level anomaly in March at all reefs
349   clustered between -0.04 and -0.08, and in September, it clustered even more tightly at -0.09 for
350   most reefs, with Pillars the sole September outlier at +0.16 m. Finally, in June, sea-level anomaly
351   ranged more widely, from a high of +0.08 at Pillars, to +0.06 at Emerald, +0.01 at Barracuda,
352   and -0.10 m at Oakland Ridge.

353 ## *Fictibacillus* and *Endozoicomonas* were dominant bacterial members in two
354 ## hard coral species in four southeast Florida reefs

355   The 55 16S rRNA amplicon sequences from coral tissue samples (24 *P. astreoides* and
356   31 *S. siderea*) were leveraged from a previous study (Staley et al. 2017). The program DADA2
357   identified a total of 22,451 ASVs and after filtering, 15,201 ASVs remained. The minimum
358   frequency of an ASV per sample was 404 and the maximum frequency was 196,536. The median
359   ASV frequency per sample was 102,667 with a mean of 98,118.
360   The microbial taxa of the samples are summarized in Fig. 4. On average, across the four
361   Southeast Florida reefs in 2015, the bacterial genus *Fictibacillus*, family *Bacillaceae* made up
362   the majority of the microbial community (N= 55; mean relative abundance, meanRA= 13.9%, ±
363   standard deviation 1.8%). The bacterial genus *Endozoicomonas*, family *Endozoicomonadaceae*
364   also had a high meanRA (12.2% ± 9.7%). When analyzing the two host-species separately, *P.*
365   *astreoides* was dominated by *Endozoicomonas* (N=24; 10.7% ± 8.0%); *S.siderea* on the other
366   hand, had a higher abundance of the genus *Fictibacillus* (N=31; 10.4% ± 11.1%), while
367   *Endozoicomonas* was only this host's 9th most abundant taxon (1.5% ± 3.0%). During the month
368   of September (N=24) specifically, across samples from both host species, the family *Bacillaceae*
369   was found at higher abundances, and was composed of the genera *Paenibacillus* (8.9% ± 12.2%)
370   and *Fictibacillus* (7.7% ± 9.6%). However, for the months of March (N=20) and June (N=11),
371   across all sites and both host species, *Endozoicomonas* showed the highest meanRA of 4.5% ±
372   5.2% (March) and 5.2% ± 9.0% (June). Two reef sites had the highest overall average
373   abundances for *Fictibacillus* across all months and both hosts: Barracuda (N=16; 4.3% ± 10.0%)
374   and Emerald (N=10; 3.8% ± 9.6%). The other two reefs showed their highest overall average
375   abundances for *Endozoicomonas* across month and host: Oakland Ridge (N=13; 4.9 % ± 8.0%)
376   and Pillars (N=16; 4.3% ± 6.8%).

377 ## Bacterial alpha diversity correlated with the physical oceanographic habitat

378   Table 1 lists three (3) categorical and 14 numerical variables. Twelve physical habitat
379   variables were selected for analysis to identify univariate correlations between these variables
380   and coral microbiomes (Overall coral cover and overall mean size were not considered; only
381   coral cover and mean size for the two host species were considered - *P. astreoides* and *S.*
382   *siderea*.). Latitude and longitude were removed from this analysis, as they correlated (ρ > 80%)
383   with other independent habitat variables.
384   Microbial Shannon diversity was negatively correlated with alongshore current speed
385   (R^2=0.05, p=0.044), tide height (R^2=0.12, p=0.004), and temperature (R^2=0.13, p=0.002; Fig.

386 5A-C). Similarly, microbial evenness was negatively correlated with sea-level (R^2=0.09,
387 p=0.014), tide height (R^2=0.12, p=0.005), and temperature (R^2 =0.15, p=0.002; Fig. 5D-F).
388 Among independent categorical variables, host species was significant to Shannon diversity
389 (p=0.04). With regard to interactions between sampling months, pairwise comparisons were
390 significant for both Shannon and evenness (p<0.05) for March vs. June and March vs.
391 September, but not for June vs. September. Finally, there were no significant pairwise
392 differences between reefs, in either Shannon diversity or evenness.

Coral bacterial community composition correlated with physical oceanographic habitat

395 In the beta-diversity analysis, ordination axis 1 of the principal coordinate analysis (PCoA)
396 explained 89.5% of the variance, and PCoA 2 explained 5.8% of the variance (Fig. 6A). Of
397 correlations between the 12 numeric habitat variables considered, and axis 1 or axis 2 of the
398 ordination, only relative turbidity was significant to axis 2 (R^2=0.27, p<0.05). In addition, for
399 categorical variables, an ANOSIM showed that the microbial community correlated with host
400 species (R^2=0.38, p=0.001) and month (R^2=0.21, p=0.001), but not with reef location (R^2=0.04,
401 p=0.094). A PERMANOVA also showed the same results for host-species (p >0.001), month (p
402 >0.001), and reef location (p=0.86). Four of the 12 habitat variables had explanatory power for
403 the microbiome count matrix: alongshore currents (p=0.005), relative turbidity (p=0.015),
404 significant wave height (p=0.005), and temperature (p=0.005). All four of these variables had a
405 variance-inflation factor (VIF, diagonal of the inverse of the correlation coefficient matrix) < 2,
406 indicating that they represent effects which are independent of one another (Salmeron et al.
407 2018).
408   The canonical or constrained correspondence analysis (CCA) ordination was constrained
409 by these four habitat variables, with CCA1 and CCA2 verified as significant by one-way
410 ANOVA. Categorical data were analyzed vs. CCA1 and CCA2: month (R^2=0.52, p=0.001) and
411 reef (R^2=0.15, p=0.009) were found to be significant, but the host species was not. Given that
412 host species was not a significant factor to CCA, we analyzed samples from both species
413 together. Accordingly, the CCA ordination plot annotated by month and reef (Fig. 6B) shows
414 that microbial communities cluster primarily by month, with samples collected in March (N= 20)
415 correlating with significant wave height and relative turbidity, and samples collected in
416 September (N=24) correlating with temperature; samples collected in June (N=11) correlated
417 with alongshore current speed.
418

Microbial taxa correlated with changes in waves and temperature

420 To identify individual microbial taxa that correlated with changes in the physical oceanographic
421 habitat, we used a Random Forest Regressor (RFR) for variable selection, and then applied a
422 simple linear regression on individual variables. Based on `ordistep` model outputs, we
423 analyzed four variables with RFR – significant wave height, relative turbidity, alongshore
424 currents, and sea temperature. The RFR classification model was significant for significant wave
425 height (p<0.001, R^2=0.85), alongshore currents (p <0.01, R^2=0.60), and sea temperature
426 (p<0.001, R^2=0.85). The model was not significant for relative turbidity (p=0.92, R^2=0.001). The
427 five microbial taxa with the highest importance values from each significant RFR model are

428 listed in Supplementary Table 1. That table also notes which of these "important" taxa were
429 significantly correlated (p <0.05, R^2 >0.2) with their respective habitat variables. For significant
430 wave height, two taxa were significant from the order *Flavobacteriale*s, and one from Marine
431 Group II. For temperature, one taxon was significantly correlated from the order SAR86 (Fig. 7).
432 There were no microbial taxa that were found to be correlated significantly with alongshore
433 currents (i.e., none with p <0.05 and R^2 >0.2).
434

Discussion

435

436   In our study, we found distinct interactions of individual physical habitat variables with
437 multiple microbiome structure variables. These physical oceanographic habitat variables do co-
438 vary with one another over a range of time and space scales. For example, water temperatures
439 can be driven by thermal advection, temperature gradients can force water flow through
440 horizontal convection, and turbidity is often the result of wave breaking. Recent published results
441 have demonstrated that indeed, the complex interaction between physical variables like flow,
442 light, and temperature may potentiate their effects on coral microbiomes (Lee et al. 2017; van
443 Oppen et al. 2018). To add to the complexity of these physical habitat factors, a combination of
444 physico-chemical components also works together to affect the microbial communities on coral
445 reefs (Roik et al. 2016). However, here, we aimed to tease apart which univariate responses of
446 the coral microbiome to individual habitat variables were significant.
447   Our results show that 95% of the variance in microbial beta-diversity was explained in
448 the first two PCoA axis, and that coral species had the highest group separation (R^2=0.38) among
449 categorical factors (i.e., month, species, reef; Fig. 6A). Coral species (*P. astreoides* and *S.*
450 *siderea*), each have a unique microbial diversity composed of different taxa (Fig. 4 and Fig. 6A).
451 However, we also found correlations across the two host species, between coral microbiomes
452 and temperature, turbidity (related to available light), and multiple scales of waterflow (i.e., those
453 related to modeled larger-scale ocean currents, smaller-scale responses to sea-level gradient, and
454 waves).
455   We found that increases in tide height, sea-level, sea temperature, and modeled
456 alongshore currents were associated with declines in microbial Shannon diversity and/or
457 evenness (Fig. 5). Among shallow coastal environments such as those on tidal flats, tide changes
458 affect the structure and function of the microbial community (Lü et al. 2016). Similarly, studies
459 of reefs below the tidal zone have shown that differing seawater depths (related to available light
460 and flow regimes) do correlate with changes in bacterial communities (Bonthond et al. 2018;
461 Klaus et al. 2007; Pantos et al. 2015). Although we found increased sea-level and tide height
462 both independently associated with decreased alpha-diversity, we cannot state which specific
463 physical process explains these results. This is because the overall range of relative water height
464 variations observed in this study from both modeled tides and direct (moored sea pressure)
465 measurements was small, 0.25 m or less than 5% of the shallowest mean site depths
466 (Supplementary Fig. S2). Hence, any influence that sea-level (including tides) had on these
467 microbiomes was more likely due to low-frequency variability in currents and/or transports
468 forced by sea-level gradients, rather than to the sea-level variations themselves. In particular,
469 low-frequency variability from both wind setup and tide can drive cross-shelf transport (Castelao
470 et al. 2010; Lee & Smith 2002; Leichter et al. 1996), affecting microbial connectivity (Sawstrom
471 et al. 2016), flushing times (Castelao et al. 2010), and the availability of prey and nutrient inputs

472   (Leichter et al. 2003; Monismith et al. 2010; O'Connell et al. 2018). Such effects may serve to
473   reduce microbial alpha-diversity on reefs (O'Connell et al. 2018) and may explain the
474   correlations we observed.
475   For beta-diversity, the four habitat variables that best describe the data were significant
476   wave height, alongshore currents, relative turbidity, and temperature. In March, microbial beta-
477   diversity was correlated (Fig. 6B) with high multi-site median relative turbidity (Fig. 3C, all
478   sites) and a range of significant wave heights between reefs (Fig. 3B, e.g., Pillars vs. Oakland
479   Ridge). Corals sampled in the present study were at bottom depths between 6 and 12 m and thus,
480   were likely to be influenced by waves of the amplitudes we found from the model (Fig. 3 and
481   Supplementary Fig. S3), both from orbital motions (Rogers et al. 2015) and wave-driven
482   circulation (Rogers et al. 2018).
483   In response to significant wave height, we found that a euryarchaeotal taxon from Marine
484   Group II decreased throughout the study period with increases in wave height (Fig. 7A).
485   Euryarchaeota are known microbiome members in corals, with the majority of this taxon
486   belonging to Marine Group II (Siboni et al. 2008). However, no study, to our knowledge, has
487   described the role played by these archaea in coral microbiomes (Bourne et al. 2016). Our
488   analysis suggests that Marine Group II may play a larger role in the coral microbiome during
489   times of lower wave activity such as June and, at some sites, in September. In March, during
490   times of higher wave activity, there was an increase in relative abundance of the bacterial order
491   *Flavobacteriales*, genus *Tenacibaculum* (Fig. 7A). The genus *Tenacibaculum* encompasses
492   bacteria that are associated with the marine environment and can be pathogenic (Park et al. 2016;
493   Smage et al. 2016). This *Tenacibaculum* ASV has a 100% sequence identity with *Tenacibaculum*
494   *sediminilitoris* - an isolate from tidal flats (Park et al. 2016). Both tidal flat sediments and
495   seawater are sources of *Tenacibaculum;* therefore, it is possible that the presence of this genus
496   during high wave activity is due to sedimentation resuspension.
497   The CI dataset is designed to map out visible influences of inshore events on coral reefs
498   using satellite ocean color data. This applies equally to plumes associated with the effects of
499   breaking waves inshore, and those potentially attributable to human activities. High turbidity on
500   the shelf can be due to waves through erosion or sediment resuspension. However, when
501   turbidity occurs in the absence of higher waves (Fig. 3B-C), as it did at some sites in March
502   (Oakland Ridge and Emerald) and again in June (Barracuda and Oakland Ridge), it is considered
503   more likely to be due to human activities such as dredging or flood control (Barnes et al. 2015;
504   Gramer & Hendee 2018). Indeed, a major port expansion was ongoing at Port of Miami,
505   approximately 9 km east-southeast of Emerald Reef, and 13, 37, and 46 km from Pillars,
506   Barracuda, and Oakland Ridge, respectively. Primary dredging on this project ended on 08 April
507   2015, with "spot" dredging that continued into September of 2015. In March alone, we see
508   historically high turbidity throughout the reefs we sampled (Fig. 3C), with a plume that includes
509   the area surrounding the outer channel of Port of Miami (Fig. 2A). Interestingly, in March data,
510   we also see a correlation between relative turbidity and coral microbiome beta diversity (Fig.
511   6B).
512   With regard to waves in September, we note that Tropical Storm Joaquin was meandering
513   over waters near the Bahamas beginning on 28 September, and had intensified to a Category 4
514   hurricane by 01 October. During the final sampling day of the present study on 28 September,
515   this storm appears to have already brought higher significant wave heights to the entire shelf,
516   which affected samples taken at both Pillars and Emerald Reef (Fig. 3B). Modification of the
517   reef environment by remote tropical systems occurs episodically in south Florida (Manzello et al.

518   2007). This result suggests that tropical weather systems impacted the physical environment of
519   these reefs via wave action (Fig. 2 and Fig. 3). However, we note that waves from this indirect
520   effect were still smaller than those from the direct effect of synoptic weather systems from the
521   previous March (Fig. 3B, all sites). The effect in September was also only sampled at two of the
522   four reefs, due to timing. Either of these differences could explain why microbiome structure
523   related to waves stood out in March, but not in September (Fig. 6).
524   A number of studies have reported that the microbial community in corals responds to
525   temperature fluctuations (McDevitt-Irwin et al. 2017; Zaneveld et al. 2016). In this study, we
526   also see that coral microbial alpha- and beta-diversity correlated with temperature, with
527   September samples in particular clustering closely together by temperature (Fig. 5 and Fig. 6B).
528   In September, we see an increase in relative abundance in SAR86 from the class
529   Gammaproteobacteria. This bacterium is found in oligotrophic environments and is known to
530   respond to temperature changes (Dupont et al. 2012). It is unknown how this bacterium may
531   affect the host's health, but it may play an important role in *P. astreoides* and *S. siderea*
532   holobiont response during times of high temperature (Cardenas et al. 2012; Pootakham et al.
533   2018).
534   The pattern of sea temperatures measured by the divers and *in situ* moorings in
535   September appears consistent with summer-time upwelling superimposed on the annual
536   "weather" cycle, rather than simple annual variability (Fig. 3A). Upwelling is known to occur
537   episodically but frequently on the east Florida shelf (Pitts & Smith 1997; Walker & Gilliam
538   2013), and has been observed to affect temperature on reefs there at a wide range of depths
539   (Gramer et al. 2018). Due to upwelling, some reefs in Florida can experience cooler water
540   temperatures in August and September than they experience in January (Leichter et al. 2006;
541   Walker & Gilliam 2013). In addition to modifying the thermal environment, upwelling can also
542   enhance the flux of soluble nutrients onto a reef (Gramer et al. 2018). Furthermore, the onset and
543   relaxation of an upwelling event may increase flushing of the shelf environment. A combination
544   of these effects from upwelling may help explain the particular relationship between temperature
545   and microbial community structure that we saw in the clustered data for September.
546

Conclusions

548   In conclusion, we identified physical oceanographic habitat variables that correlate with
549   structure in the microbiomes of two hard coral species on four urban-impacted reefs. Our study,
550   also identified summer upwelling at some of these reef sites, which decreased bottom sea
551   temperatures and may explain some aspects of the observed microbiome structure. The study
552   design, together with our use of regional-scale model and satellite data to characterize the
553   physical habitat, did not allow for lower bounds to be determined on the significant
554   (decorrelation) distances and time scales associated with variability in that habitat, nor the scales
555   of the diversity in the coral microbiomes. Our study, nonetheless, indicates potentially important
556   future considerations for improving coral health and outplant success in Florida reefs. This
557   suggests that targeted, fine-scale future studies should be conducted at outplant sites, combining
558   continuous physical measurements with repeated surveys and biological sampling, in order to
559   further establish the relative importance of various oceanographic habitat characteristics in
560   determining microbiology, coral health, and restoration success.

References

561

562 Barnes BB, Hu CM, Kovach C, and Silverstein RN. 2015. Sediment plumes induced by the Port
563   of Miami dredging: Analysis and interpretation using Landsat and MODIS data. *Remote*
564   *Sensing of Environment* 170:328-339. 10.1016/j.rse.2015.09.023
565 Baums IB, Paris CB, and Cherubin LM. 2006. A bio-oceanographic filter to larval dispersal in a
566   reef-building coral. *Limnology and Oceanography* 51:1969-1981.
567 Bayraktarov E, Pizarro V, Eidens C, Wilke T, and Wild C. 2013. Bleaching susceptibility and
568   recovery of Colombian Caribbean corals in response to water current exposure and
569   seasonal upwelling. *Plos One* 8:11. 10.1371/journal.pone.0080536
570 Boehm AB, Lluch-Cota DB, Davis KA, Winant CD, and Monismith SG. 2004. Covariation of
571   coastal water temperature and microbial pollution at interannual to tidal periods.
572   *Geophysical Research Letters* 31. L06309 10.1029/2003gl019122
573 Bonthond G, Merselis DG, Dougan KE, Graff T, Todd W, Fourqurean JW, and Rodriguez-
574   Lanetty M. 2018. Inter-domain microbial diversity within the coral holobiont Siderastrea
575   siderea from two depth habitats. *Peerj* 6:25. 10.7717/peerj.4323
576 Bourne D, Iida Y, Uthicke S, and Smith-Keune C. 2008. Changes in coral-associated microbial
577   communities during a bleaching event. *Isme Journal* 2:350-363. 10.1038/ismej.2007.112
578 Bourne DG, Morrow KM, and Webster NS. 2016. Insights into the Coral Microbiome:
579   Underpinning the Health and Resilience of Reef Ecosystems. In: Gottesman S, ed.
580   Annual Review of Microbiology, Vol 70. Palo Alto: Annual Reviews, 317-340
581 Callahan BJ, McMurdie PJ, Rosen MJ, Han AW, Johnson AJA, and Holmes SP. 2016. DADA2:
582   High-resolution sample inference from Illumina amplicon data. *Nature Methods* 13:581-
583   +. 10.1038/nmeth.3869
584 Cardenas A, Rodriguez LM, Pizarro V, Cadavid LF, and Arevalo-Ferro C. 2012. Shifts in
585   bacterial communities of two caribbean reef-building coral species affected by white
586   plague disease. Isme Journal 6:502-512. 10.1038/ismej.2011.123
587 Carignan KS, McLean SJ, Eakins BW, Beasley L, Love MR, and Sutherland M. 2015. Digital
588   Elevation Model of Miami, Florida: Procedures, data sources, and analysis. NOAA
589   Technical Report. Boulder, CO: National Geophysical Data Center. p 11 pp.
590 Castelao R, Chant R, Glenn S, and Schofield O. 2010. The effects of tides and oscillatory winds
591   on the subtidal inner-shelf cross-shelf circulation. *Journal of Physical Oceanography*
592   40:775-788. 10.1175/2009jpo4273.1
593 Clarke KR, and Warwick RM. 1994. Similarity-based testing for community pattern - The 2-way
594   layout with no replication. *Marine Biology* 118:167-176. 10.1007/bf00699231
595 Cushman-Roisin B, and Beckers J-M. 2011. *Introduction to Geophysical Fluid Dynamics:*
596   *Physical and Numerical Aspects*: Academic Press.
597 Davis KA, Lentz SJ, Pineda J, Farrar JT, Starczak VR, and Churchill JH. 2011. Observations of
598   the thermal environment on Red Sea platform reefs: a heat budget analysis. *Coral Reefs*
599   30:25-36. 10.1007/s00338-011-0740-8
600 Drury C, Schopmeyer S, Goergen E, Bartels E, Nedimyer K, Johnson M, Maxwell K, Galvan V,
601   Manfrino C, and Lirman D. 2017. Genomic patterns in Acropora cervicornis show
602   extensive population structure and variable genetic diversity. *Ecology and Evolution*
603   7:6188-6200. 10.1002/ece3.3184
604 Dupont CL, Rusch DB, Yooseph S, Lombardo MJ, Richter RA, Valas R, Novotny M, Yee-
605   Greenbaum J, Selengut JD, Haft DH, Halpern AL, Lasken RS, Nealson K, Friedman R,

606   and Venter JC. 2012. Genomic insights to SAR86, an abundant and uncultivated marine
607   bacterial lineage. Isme Journal 6:1186-1199. 10.1038/ismej.2011.189
608 Edmunds PJ. 2010. Population biology of Porites astreoides and Diploria strigosa on a shallow
609   Caribbean reef. *Marine Ecology Progress Series* 418:87-U508. 10.3354/meps08823
610 Feng M, Colberg F, Slawinski D, Berry O, and Babcock R. 2016a. Ocean circulation drives
611   heterogeneous recruitments and connectivity among coral populations on the North West
612   Shelf of Australia. *Journal of Marine Systems* 164:1-12. 10.1016/j.jmarsys.2016.08.001
613 Feng ZX, Reniers A, Haus BK, Solo-Gabriele HM, and Kelly EA. 2016b. Wave energy level and
614   geographic setting correlate with Florida beach water quality. *Marine Pollution Bulletin*
615   104:54-60. 10.1016/j.marpolbul.2016.02.011
616 Gierach MM, Subrahmanyam B, and Thoppil PG. 2009. Physical and biological responses to
617   Hurricane Katrina (2005) in a 1/25 degrees nested Gulf of Mexico HYCOM. *Journal of*
618   *Marine Systems* 78:168-179. 10.1016/j.jmarsys.2009.05.002
619 Gilliam DS. 2009. Southeast Florida Coral Reef Evaluation and Monitoring Project 2008 Year 6
620   Final Report. Miami Beach, FL: Florida DEP Report. p 39.
621 Gischler E, Storz D, and Schmitt D. 2014. Sizes, shapes, and patterns of coral reefs in the
622   Maldives, Indian Ocean: the influence of wind, storms, and precipitation on a major
623   tropical carbonate platform. *Carbonates and Evaporites* 29:73-87. 10.1007/s13146-013-
624   0176-z
625 Glasl B, Herndl GJ, and Frade PR. 2016. The microbiome of coral surface mucus has a key role
626   in mediating holobiont health and survival upon disturbance. *Isme Journal* 10:2280-2292.
627   10.1038/ismej.2016.9
628 Gramer LJ. 2013. The dynamics of sea temperature variability on Florida's reef tract Ph.D.
629   University of Miami Rosenstiel School of Marine and Atmospheric Studies.
630 Gramer LJ, and Hendee JC. 2018. Coastal turbidity on the southeast Florida shelf: Monitoring
631   turbid water sources and fates by satellite. NOAA Technical Memorandum OAR-
632   AOML-105. Miami, FL, USA: NOAA-AOML. p 46 pp.
633 Gramer LJ, Hendee JC, Stamates SJ, Walker BK, Walter RK, and Coleman DJ. 2018. Upwelling
634   on the southeast Florida shelf: Summer sea temperature extremes and associated nutrient
635   fluxes over a 17 year period. NOAA Technical Memorandum OAR-AOML-107. Miami,
636   FL, USA: NOAA AOML. p 45 pp.
637 Gregr EJ, and Bodtker KM. 2007. Adaptive classification of marine ecosystems: Identifying
638   biologically meaningful regions in the marine environment. *Deep-Sea Research Part I-*
639   *Oceanographic Research Papers* 54:385-402. 10.1016/j.dsr.2006.11.004
640 Harborne AR, Mumby PJ, Zychaluk K, Hedley JD, and Blackwell PG. 2006. Modeling the beta
641   diversity of coral reefs. *Ecology* 87:2871-2881. 10.1890/0012-
642   9658(2006)87[2871:mtbdoc]2.0.co;2
643 Hearn CJ, Atkinson MJ, and Falter JL. 2001. A physical derivation of nutrient-uptake rates in
644   coral reefs: effects of roughness and waves. *Coral Reefs* 20:347-356. 10.1007/s00338-
645   001-0185-6
646 Henriques IS, Alves A, Tacao M, Almeida A, Cunha A, and Correia A. 2006. Seasonal and
647   spatial variability of free-living bacterial community composition along an estuarine
648   gradient (Ria de Aveiro, Portugal). *Estuarine Coastal and Shelf Science* 68:139-148.
649   10.1016/j.ecss.2006.01.015
650 Kelly LW, Williams GJ, Barott KL, Carlson CA, Dinsdale EA, Edwards RA, Haas AF, Haynes
651   M, Lim YW, McDole T, Nelson CE, Sala E, Sandin SA, Smith JE, Vermeij MJA, Youle

652   M, and Rohwer F. 2014. Local genomic adaptation of coral reef-associated microbiomes
653   to gradients of natural variability and anthropogenic stressors. *Proceedings of the*
654   *National Academy of Sciences of the United States of America* 111:10227-10232.
655   10.1073/pnas.1403319111
656 Kench PS, and Brander RW. 2006. Wave processes on coral reef flats: Implications for reef
657   geomorphology using Australian case studies. *Journal of Coastal Research* 22:209-223.
658   10.2112/05a-0016.1
659 Kimes NE, Van Nostrand JD, Weil E, Zhou JZ, and Morris PJ. 2010. Microbial functional
660   structure of Montastraea faveolata, an important Caribbean reef-building coral, differs
661   between healthy and yellow-band diseased colonies. *Environmental Microbiology*
662   12:541-556. 10.1111/j.1462-2920.2009.02113.x
663 Klaus JS, Janse I, Heikoop JM, Sanford RA, and Fouke BW. 2007. Coral microbial
664   communities, zooxanthellae and mucus along gradients of seawater depth and coastal
665   pollution. *Environmental Microbiology* 9:1291-1305. 10.1111/j.1462-2920.2007.01249.x
666 Lee BC, Fan YM, Chuang LZH, and Kao CC. 2009. Parametric Sensitivity Analysis of the
667   WAVEWATCH III Model. *Terrestrial Atmospheric and Oceanic Sciences* 20:425-432.
668   10.3319/TAO.2008.04.25.01(Oc)
669 Lee STM, Davy SK, Tang SL, and Kench PS. 2017. Water flow buffers shifts in bacterial
670   community structure in heat-stressed Acropora muricata. *Scientific Reports* 7:13.
671   10.1038/srep43600
672 Lee TN, and Smith N. 2002. Volume transport variability through the Florida Keys tidal
673   channels. *Continental Shelf Research* 22:1361-1377.
674 Leichter JJ, Helmuth B, and Fischer AM. 2006. Variation beneath the surface: Quantifying
675   complex thermal environments on coral reefs in the Caribbean, Bahamas and Florida.
676   *Journal of Marine Research* 64:563-588.
677 Leichter JJ, Stewart HL, and Miller SL. 2003. Episodic nutrient transport to Florida coral reefs.
678   *Limnology and Oceanography* 48:1394-1407.
679 Leichter JJ, Wing SR, Miller SL, and Denny MW. 1996. Pulsed delivery of subthermocline
680   water to Conch Reef (Florida Keys) by internal tidal bores. *Limnology and*
681   *Oceanography* 41:1490-1501.
682 Lirman D, and Schopmeyer S. 2016. Ecological solutions to reef degradation: optimizing coral
683   reef restoration in the Caribbean and Western Atlantic. *Peerj* 4:19. 10.7717/peerj.2597
684 Lirman D, Schopmeyer S, Manzello D, Gramer LJ, Precht WF, Muller-Karger F, Banks K,
685   Barnes B, Bartels E, Bourque A, Byrne J, Donahue S, Duquesnel J, Fisher L, Gilliam D,
686   Hendee J, Johnson M, Maxwell K, McDevitt E, Monty J, Rueda D, Ruzicka R, and
687   Thanner S. 2011. Severe 2010 cold-water event caused unprecedented mortality to corals
688   of the Florida reef tract and reversed previous survivorship patterns. *Plos One* 6:e23047.
689   e23047 10.1371/journal.pone.0023047
690 Lowe RJ, and Falter JL. 2015. Oceanic Forcing of Coral Reefs. In: Carlson CA, and Giovannoni
691   SJ, eds. *Annual Review of Marine Science, Vol 7*. Palo Alto: Annual Reviews, 43-66.
692 Lozupone C, and Knight R. 2005. UniFrac: a new phylogenetic method for comparing microbial
693   communities. *Applied and Environmental Microbiology* 71:8228-8235.
694   10.1128/aem.71.12.8228-8235.2005
695 Lü XF, Ma B, Yu JB, Chang SX, Xu JM, Li YZ, Wang GM, Han GX, Bo G, and Chu XJ. 2016.
696   Bacterial community structure and function shift along a successional series of tidal flats
697   in the Yellow River Delta. *Scientific Reports* 6:10. 10.1038/srep36550

698   Manzello DP, Brandt M, Smith TB, Lirman D, Hendee JC, and Nemeth RS. 2007. Hurricanes
699   benefit bleached corals. Proceedings of the National Academy of Sciences of the United
700   States of America 104:12035-12039. 10.1073/pnas.0701194104
701   McDevitt-Irwin JM, Baum JK, Garren M, and Vega Thurber RL. 2017. Responses of coral-
702   associated bacterial communities to local and global stressors. *Frontiers in Marine*
703   *Science* 4:262.
704   Monismith SG, Barkdull MK, Nunome Y, and Mitarai S. 2018. Transport Between Palau and the
705   Eastern Coral Triangle: Larval Connectivity or Near Misses. *Geophysical Research*
706   *Letters* 45:4974-4981. 10.1029/2018gl077493
707   Monismith SG, Davis KA, Shellenbarger GG, Hench JL, Nidzieko NJ, Santoro AE, Reidenbach
708   MA, Rosman JH, Holtzman R, Martens CS, Lindquist NL, Southwell MW, and Genin A.
709   2010. Flow effects on benthic grazing on phytoplankton by a Caribbean reef. *Limnology*
710   *and Oceanography* 55:1881-1892. 10.4319/lo.2010.55.5.1881
711   O'Connell L, Gao S, McCorquodale D, Fleisher J, and Lopez JV. 2018. Fine grained
712   compositional analysis of Port Everglades Inlet microbiome using high throughput DNA
713   sequencing. *Peerj* 6:21. 10.7717/peerj.4671
714   Pantos O, Bongaerts P, Dennis PG, Tyson GW, and Hoegh-Guldberg O. 2015. Habitat-specific
715   environmental conditions primarily control the microbiomes of the coral *Seriatopora*
716   *hystrix*. *Isme Journal* 9:1916-1927. 10.1038/ismej.2015.3
717   Park S, Ha MJ, Jung YT, Kang CH, and Yoon JH. 2016. Tenacibaculum sediminilitoris sp nov.,
718   isolated from a tidal flat. International Journal of Systematic and Evolutionary
719   Microbiology 66:2610-2616. 10.1099/ijsem.0.001086
720   Pitts PA, and Smith NP. 1997. An investigation of summer upwelling across central Florida's
721   Atlantic coast: The case for wind stress forcing. *Journal of Coastal Research* 13:105-110.
722   Pootakham W, Mhuantong W, Putchim L, Yoocha T, Sonthirod C, Kongkachana W,
723   Sangsrakru D, Naktang C, Jomchai N, Thongtham N, and Tangphatsornruang S. 2018.
724   Dynamics of coral-associated microbiomes during a thermal bleaching event.
725   Microbiologyopen 7. 10.1002/mbo3.604
726   Porter SN, Branch GM, and Sink KJ. 2017. Changes in shallow-reef community composition
727   along environmental gradients on the East African coast. *Marine Biology* 164.
728   10.1007/s00227-017-3130-0
729   Robinson MD, McCarthy DJ, and Smyth GK. 2010. edgeR: a Bioconductor package for
730   differential expression analysis of digital gene expression data. *Bioinformatics* 26:139-
731   140. 10.1093/bioinformatics/btp616
732   Roder C, Arif C, Daniels C, Weil E, and Voolstra CR. 2014. Bacterial profiling of White Plague
733   Disease across corals and oceans indicates a conserved and distinct disease microbiome.
734   *Molecular Ecology* 23:965-974. 10.1111/mec.12638
735   Rogers JS, Maticka SA, Chirayath V, Woodson CB, Alonso JJ, and Monismith SG. 2018.
736   Connecting Flow over Complex Terrain to Hydrodynamic Roughness on a Coral Reef.
737   *Journal of Physical Oceanography* 48:1567-1587. 10.1175/jpo-d-18-0013.1
738   Rogers JS, Monismith SG, Dunbar RB, and Koweek D. 2015. Field observations of wave-driven
739   circulation over spur and groove formations on a coral reef. *Journal of Geophysical*
740   *Research-Oceans* 120:145-160. 10.1002/2014jc010464
741   Rogers JS, Monismith SG, Feddersen F, and Storlazzi CD. 2013. Hydrodynamics of spur and
742   groove formations on a coral reef. *Journal of Geophysical Research-Oceans* 118:3059-
743   3073. 10.1002/jgrc.20225

744   Roik A, Rothig T, Roder C, Ziegler M, Kremb SG, and Voolstra CR. 2016. Year-Long
745   Monitoring of Physico-Chemical and Biological Variables Provide a Comparative
746   Baseline of Coral Reef Functioning in the Central Red Sea. Plos One 11.
747   10.1371/journal.pone.0163939
748   Salmeron R, Garcia CB, and Garcia J. 2018. Variance Inflation Factor and Condition Number in
749   multiple linear regression. *Journal of Statistical Computation and Simulation* 88:2365-
750   2384. 10.1080/00949655.2018.1463376
751   Sawstrom C, Hyndes GA, Eyre BD, Huggett MJ, Fraser MW, Lavery PS, Thomson PG,
752   Tarquinio F, Steinberg PD, and Laverock B. 2016. Coastal connectivity and spatial
753   subsidy from a microbial perspective. *Ecology and Evolution* 6:6662-6671.
754   10.1002/ece3.2408
755   Serrano X, Baums IB, O'Reilly K, Smith TB, Jones RJ, Shearer TL, Nunes FLD, and Baker AC.
756   2014. Geographic differences in vertical connectivity in the Caribbean coral Montastraea
757   cavernosa despite high levels of horizontal connectivity at shallow depths. *Molecular*
758   *Ecology* 23:4226-4240. 10.1111/mec.12861
759   Serrano XM, Baums IB, Smith TB, Jones RJ, Shearer TL, and Baker AC. 2016. Long distance
760   dispersal and vertical gene flow in the Caribbean brooding coral Porites astreoides.
761   *Scientific Reports* 6:12. 10.1038/srep21619
762   Shedrawi G, Falter JL, Friedman KJ, Lowe RJ, Pratchett MS, Simpson CJ, Speed CW, Wilson
763   SK, and Zhang ZL. 2017. Localised hydrodynamics influence vulnerability of coral
764   communities to environmental disturbances. *Coral Reefs* 36:861-872. 10.1007/s00338-
765   017-1576-7
766   Siboni N, Ben-Dov E, Sivan A, and Kushmaro A. 2008. Global distribution and diversity of
767   coral-associated Archaea and their possible role in the coral holobiont nitrogen cycle.
768   Environmental Microbiology 10:2979-2990. 10.1111/j.1462-2920.2008.01718.x
769   Sinigalliano CD, Carsey TP, Enochs IC, Featherstone CM, Gidley ML, Gramer LJ, Jones PR,
770   Rosales SM, Staley C, and Stamates SJ. 2018. Water quality and coral reef monitoring
771   along the southeast Florida coast. NOAA Technical Memorandum OAR-AOML-47.
772   Miami, FL, USA: NOAA-AOML. p 145 pp.
773   Smage SB, Brevik OJ, Duesund H, Ottem KF, Watanabe K, and Nylund A. 2016.
774   Tenacibaculum finnmarkense sp nov., a fish pathogenic bacterium of the family
775   Flavobacteriaceae isolated from Atlantic salmon. Antonie Van Leeuwenhoek
776   International Journal of General and Molecular Microbiology 109:273-285.
777   10.1007/s10482-015-0630-0
778   Sponaugle S, Lee T, Kourafalou V, and Pinkard D. 2005. Florida current frontal eddies and the
779   settlement of coral reef fishes. *Limnology and Oceanography* 50:1033-1048.
780   Staley C, Kaiser T, Gidley ML, Enochs IC, Jones PR, Goodwin KD, Sinigalliano CD, Sadowsky
781   MJ, and Chun CL. 2017. Differential Impacts of Land-Based Sources of Pollution on the
782   Microbiota of Southeast Florida Coral Reefs. *Applied and Environmental Microbiology*
783   83:16. 10.1128/aem.03378-16
784   Stammer D, Ray RD, Andersen OB, Arbic BK, Bosch W, Carrere L, Cheng Y, Chinn DS,
785   Dushaw BD, Egbert GD, Erofeeva SY, Fok HS, Green JAM, Griffiths S, King MA,
786   Lapin V, Lemoine FG, Luthcke SB, Lyard F, Morison J, Muller M, Padman L, Richman
787   JG, Shriver JF, Shum CK, Taguchi E, and Yi Y. 2014. Accuracy assessment of global
788   barotropic ocean tide models. *Reviews of Geophysics* 52:243-282. 10.1002/2014rg000450

789   Sweet MJ, Brown BE, Dunne RP, Singleton I, and Bulling M. 2017. Evidence for rapid, tide-
790   related shifts in the microbiome of the coral *Coelastrea aspera*. *Coral Reefs* 36:815-828.
791   10.1007/s00338-017-1572-y
792   Tkachenko KS, and Soong K. 2017. Dongsha Atoll: A potential thermal refuge for reef-building
793   corals in the South China Sea. *Marine Environmental Research* 127:112-125.
794   10.1016/j.marenvres.2017.04.003
795   Tolman HL. 2014. User manual and system documentation of WAVEWATCH III R version
796   4.07. NOAA/NWS/NCEP/MMAB Tech. Note 222.
797   van Oppen MJH, Bongaerts P, Frade P, Peplow L, Boyd SE, Nim HT, and Bay LK. 2018.
798   Adaptation to reef habitats through selection on the coral animal and its associated
799   microbiome. *Molecular Ecology* 27:2956-2971. 10.1111/mec.14763
800   Walker BK, and Gilliam DS. 2013. Determining the Extent and Characterizing Coral Reef
801   Habitats of the Northern Latitudes of the Florida Reef Tract (Martin County). *Plos One* 8.
802   10.1371/journal.pone.0080439
803   Walton CJ, Hayes NK, and Gilliam DS. 2018. Impacts of a regional, multi-year, multi-species
804   coral disease outbreak in southeast Florida. *Frontiers in Marine Science* 5:14.
805   10.3389/fmars.2018.00323
806   Young CN, Schopmeyer SA, and Lirman D. 2012. A review of reef restoration and coral
807   propagation using the threatened genus *Acropora* in the Caribbean and Western Atlantic.
808   *Bulletin of Marine Science* 88:1075-1098. 10.5343/bms.2011.1143
809   Zaneveld JR, Burkepile DE, Shantz AA, Pritchard CE, McMinds R, Payet JP, Welsh R, Correa
810   AMS, Lemoine NP, Rosales S, Fuchs C, Maynard JA, and Thurber RV. 2016.
811   Overfishing and nutrient pollution interact with temperature to disrupt coral reefs down to
812   microbial scales. *Nature Communications* 7:12. 10.1038/ncomms11833
813   Zhang ZL, Lowe R, Falter J, and Ivey G. 2011. A numerical model of wave- and current-driven
814   nutrient uptake by coral reef communities. *Ecological Modelling* 222:1456-1470.
815   10.1016/j.ecolmodel.2011.01.014
816   Ziegler M, Roik A, Porter A, Zubier K, Mudarris MS, Ormond R, and Voolstra CR. 2016. Coral
817   microbial community dynamics in response to anthropogenic impacts near a major city in
818   the central Red Sea. *Marine Pollution Bulletin* 105:629-640.
819   10.1016/j.marpolbul.2015.12.045
820   Ziegler M, Seneca FO, Yum LK, Palumbi SR, and Voolstra CR. 2017. Bacterial community
821   dynamics are linked to patterns of coral heat tolerance. *Nature Communications* 8:8.
822   10.1038/ncomms14213
823

824

List of categorical variables and continuous variable medians that were correlated with coral microbiota.

Only % coral cover and mean coral size of the overall reef were not used in the analysis.

Reef	Month	Species	N	% Coral cover cm²	μ coral size cm³	% Coral cover for SS and PA cm²	μ Coral Size for SS and PA cm³	Depth [m]	Sea floor slope	Min. dive watch temp [°C]	Dist. to nearest Inlet [km]	Relative Turbidity	Sig. Wave Height [m]	M_m tide stage [m]	Sea level [m]	Along-shore current [m/s]	Cross-shore current [m/s]
Barracuda	Mar.	PA	2	1.97	354	0.209	130.1	-9.76	0.037	23.2	2.470	-0.068	0.277	-0.0080	-0.050	0.346	-0.050
Barracuda	Jun.	PA	2	2.01	343	0.264	129.75	-9.76	0.037	28.2	2.470	0.142	0.180	0.0008	0.007	0.475	-0.077
Barracuda	Sept.	PA	2	1.5	333.8	0.262	132.73	-9.76	0.037	29.2	2.470	-0.478	0.074	-0.0058	-0.091	0.329	-0.084
Barracuda	Mar.	SS	4	1.97	354	0.209	156.33	-10.07	0.031	23.4	2.029	-0.060	0.254	-0.0080	-0.050	0.341	-0.045
Barracuda	Jun.	SS	2	2.01	343	0.264	129.75	-10.15	0.031	28.2	2.317	0.143	0.176	0.0008	0.007	0.470	-0.081
Barracuda	Sept.	SS	4	1.5	333.8	0.262	127.25	-10.07	0.031	29	2.029	-0.383	0.068	-0.0058	-0.091	0.325	-0.072
Emerald	Mar.	PA	1	1.33	261.2	0.169	232.33	-7.25	0.024	24	10.183	-0.075	0.258	-0.0052	-0.075	0.445	0.036
Emerald	Jun.	PA	1	1.28	209.5	0.193	93.75	-7.25	0.024	28	10.183	-0.426	0.182	0.0016	0.064	0.614	0.040
Emerald	Sept.	PA	3	1.17	198.8	0.205	230.5	-8.48	0.022	29.2	10.528	-0.379	0.225	0.0003	0.155	0.377	0.031
Emerald	Mar.	SS	1	1.33	261.2	0.169	101.86	-7.25	0.024	24	10.183	-0.075	0.258	-0.0052	-0.075	0.445	0.036
Emerald	Jun.	SS	1	1.28	209.5	0.193	93.75	-7.25	0.024	28	10.183	-0.426	0.182	0.0016	0.064	0.614	0.040
Emerald	Sept.	SS	3	1.17	198.8	0.205	87.5	-8.48	0.022	29.2	10.528	-0.379	0.225	0.0003	0.155	0.377	0.031
Oakland Ridge	Mar.	PA	3	2.34	186.2	0.463	223.5	-8.59	0.048	22.4	7.206	-0.089	0.255	-0.0076	-0.049	0.259	-0.001
Oakland Ridge	Jun.	PA	1	2.37	199.9	0.519	161.71	-8.67	0.048	28	7.206	0.110	0.143	-0.0050	-0.104	0.302	0.026
Oakland Ridge	Sept.	PA	3	2.31	193.8	0.519	219.67	-8.59	0.048	28.8	7.206	-0.141	0.067	-0.0043	-0.088	0.245	0.023
Oakland Ridge	Mar.	SS	3	2.34	186.2	0.463	171.07	-8.59	0.048	22.4	7.206	-0.089	0.255	-0.0076	-0.049	0.259	-0.001
Oakland Ridge	Sept.	SS	3	2.31	193.8	0.519	161.71	-8.59	0.048	28.8	7.206	-0.141	0.067	-0.0043	-0.088	0.245	0.023
Pillars	Mar.	PA	2	1.36	244.5	0.192	126.5	-10.31	0.014	23.2	4.784	-0.128	0.310	-0.0065	-0.062	0.310	-0.024
Pillars	Jun.	PA	2	1.03	300.9	0.134	162	-10.31	0.014	28	4.784	-0.164	0.183	0.0021	0.075	0.406	-0.021
Pillars	Sept.	PA	2	0.97	290.3	0.149	101	-10.31	0.014	30.2	4.784	-0.089	0.253	0.0005	0.155	0.238	0.000
Pillars	Mar.	SS	4	1.36	244.5	0.192	269	-10.92	0.015	23.8	4.531	-0.121	0.327	-0.0065	-0.062	0.310	-0.006
Pillars	Jun.	SS	2	1.03	300.9	0.134	162	-11.49	0.015	28	4.412	-0.172	0.201	0.0021	0.075	0.405	0.007
Pillars	Sept.	SS	4	0.97	290.3	0.149	205.6	-10.92	0.015	30	4.531	-0.088	0.267	0.0005	0.155	0.238	0.013

1 N is the number of replicates (distinct coral heads) of that host species sampled at that reef in that month. SS =*Siderastrea siderea* and
2 PA= *Porites astreoides.*

Figure 1

Geography of the study region.

(A) Wider geography of the Florida reef tract, showing boundaries of southern Florida counties. Sampling sites are shown as colored markers offshore of Miami-Dade and Broward counties. Grey contours show the 10, 30, and 250 m isobath. (B) High resolution bathymetry of the sampling region, showing southeast Florida's coastline in heavy black, sampling sites as colored markers, and isobaths as color contours at 3 m depth intervals down to 30 m, followed by the 40, 50, and 60 m isobaths offshore. The high resolution of this bathymetry highlights the linear, north-south features of south Florida reefs, as well as major man-made channels cut across them: Port of Miami at 25.76, Haulover at 25.90, and Port Everglades at 26.09 °N latitude.
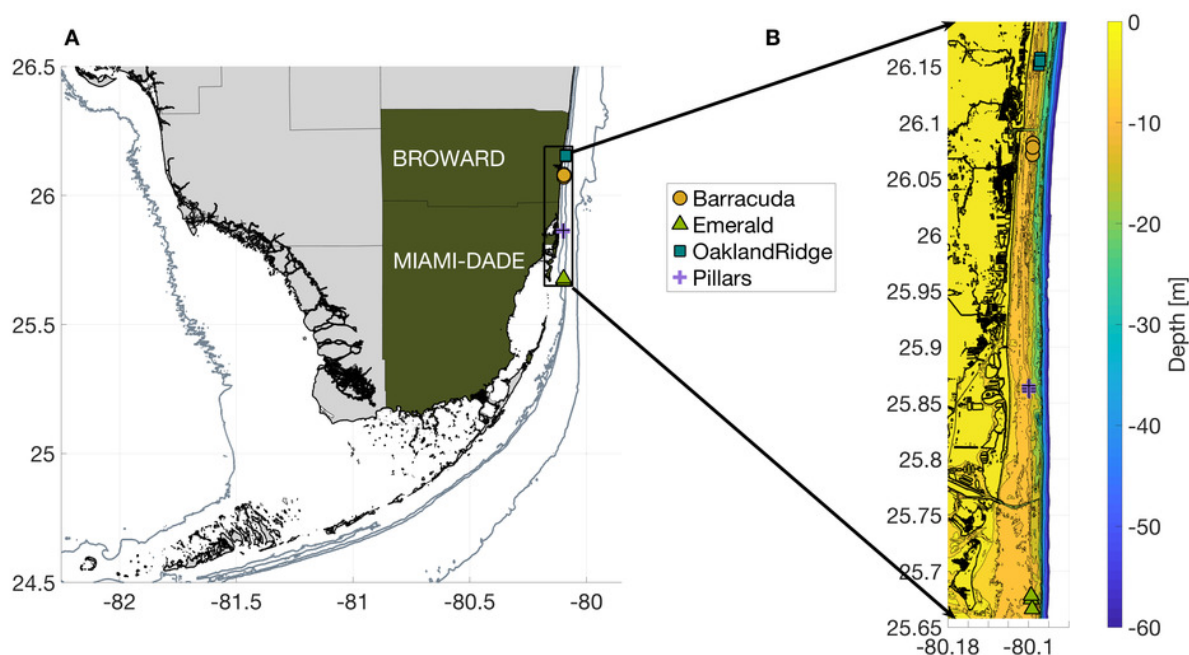
Figure 2

Physical habitat spatial fields, with time-averaged across the full weeks surrounding each sampling period.

In (A, D) March, (B, E) June, and (C, F) September. Panels (A-C) show normalized relative turbidity from satellite, and (D-F) show alongshore current [m s^{-1}] from GoM HYCOM. In (D-F), alongshore current speed (v) is shown as colored contours, and overall current direction is shown as scaled black arrows at the native model resolution. Locations of the twelve individual coral sampling sites are shown with markers, colored by reef name.
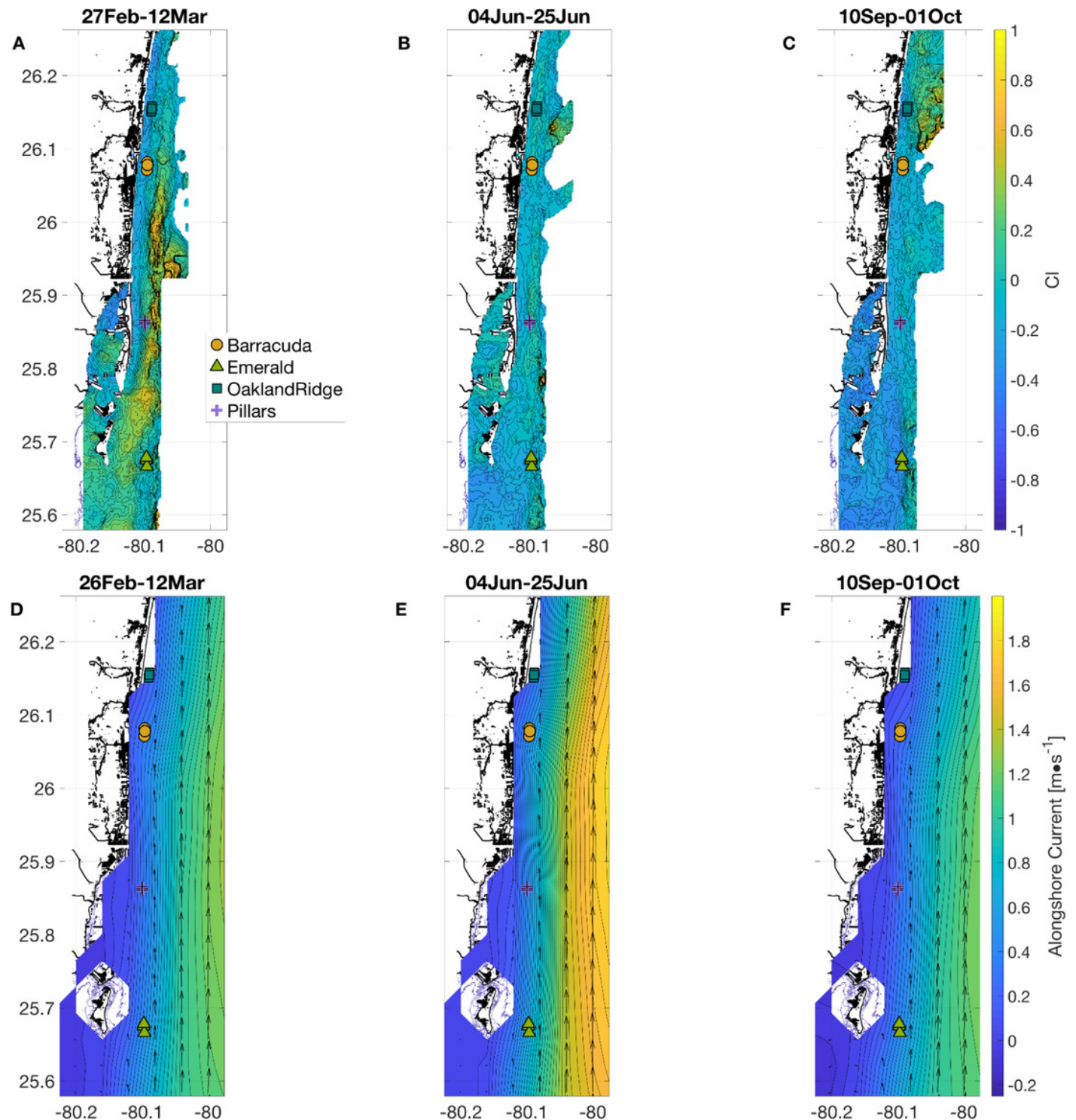
Figure 3

Physical habitat time series for 2015 at four reefs.

Reefs are marked by different shapes and dates of sampling are shown as colored markers: (A) per-dive minimum measured sea temperature [°C] from divers, and for comparison, from *in situ* moorings inshore of (black line, at 7 m depth) and offshore of (gray line, at 26 m depth) the reef lines, as well as from a dockside station (dark red line, depth about 2 m) approximately 10 km inshore. (B) The 14 d centered moving average of significant wave height [m] from NOAA WaveWatch III surface wave model, at the grid point where each sample was gathered. (C) The 14 d centered moving average of normalized relative turbidity from satellite ocean color at the pixel where each sample was gathered. (D) The 14 d centered moving average of alongshore current [m s^{-1}] from GoM HYCOM linearly interpolated to the location where each sample was gathered. The Low-pass (40-hour) filtered time series (40HLP) of measured depth-averaged ocean currents are shown in black for moorings immediately inshore (7 m depth, solid) and offshore (26 m depth, dashed) of the major reef line.
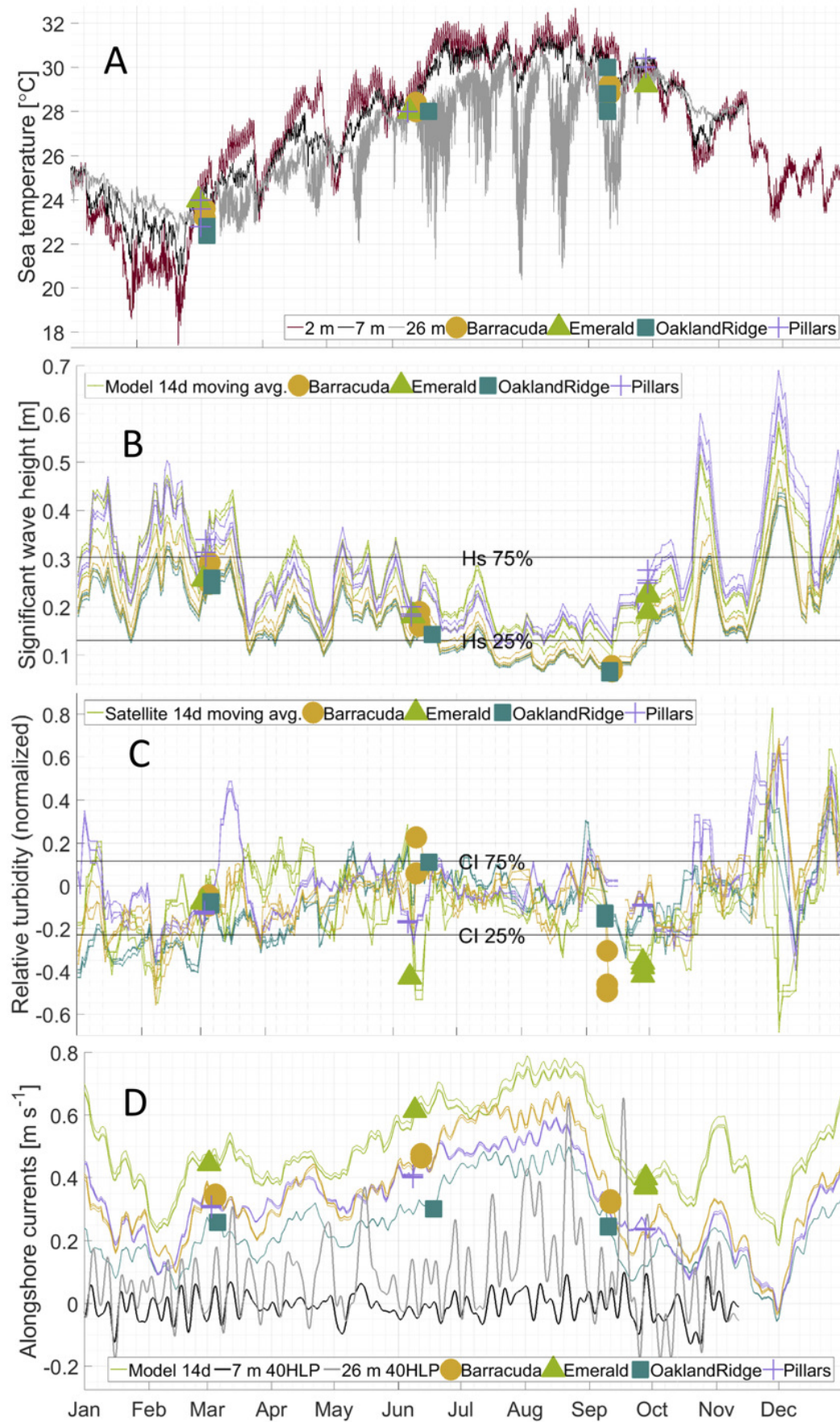
Figure 4

Relative abundance of microbial communities of *Siderastrea siderea* and *Porites astreoides* tissue from four Southeast Florida reefs.

Stacked bar colors indicate different genera and the relative abundance of each genus of the most abundant (>0.05%) ASVs. The figure is grouped by reef site, the month of sampling, and the host-species.
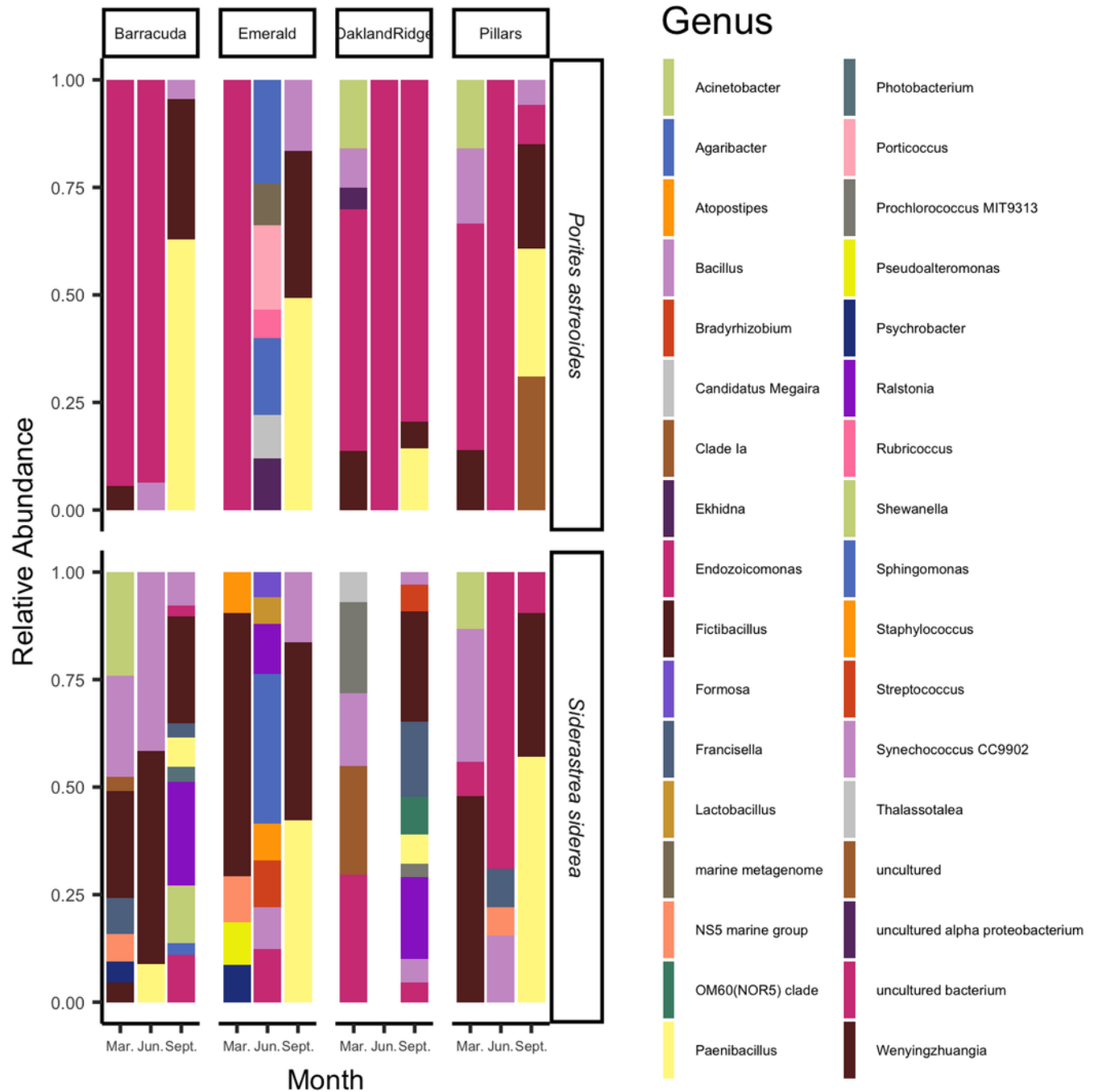
Figure 5

Microbial alpha-diversity from coral species *Siderastrea siderea* and *Porites astreoides* from four Southeast Florida reefs.

Samples are colored by month and shaped by the reef name. The blue line represents the linear regression best fit between the habitat variable (x axis) and the diversity metric (y axis); grey shadow around the blue line is the 95% confidence interval. The first column plots Shannon diversity vs. physical habitat variables that were found to be significant to it ($p <$ 0.05) (A) alongshore currents [m s^{-1}], (B) tide [m], and (C) temperature [°C]. The second column of plots show species evenness of habitat vs. variables that were significant ($p <$ 0.05) (D) sea-level anomaly [m], (E) tide [m], and (F) temperature [°C].
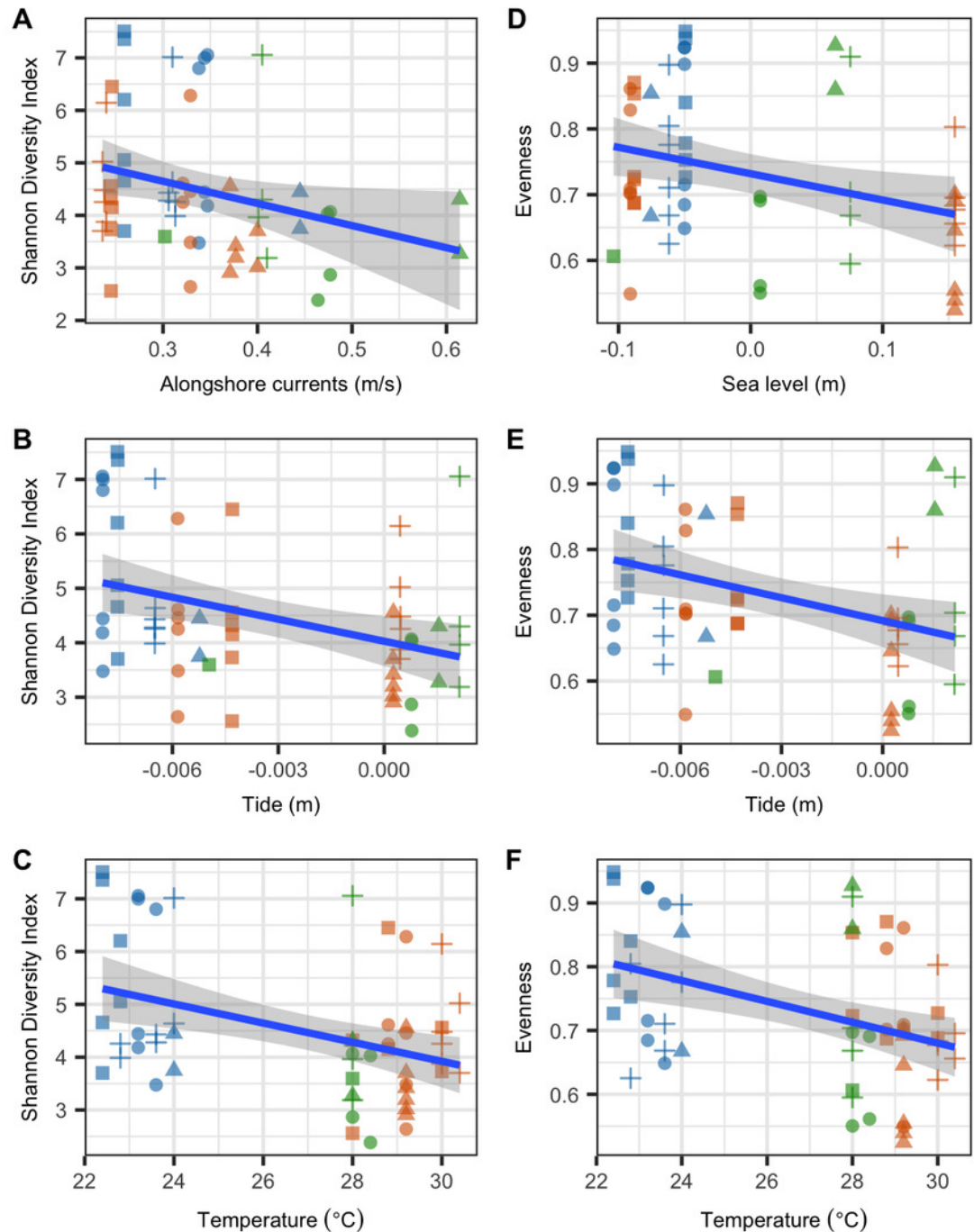
Figure 6

Microbial beta-diversity of coral *Siderastrea siderea* (SS) and *Porites astreoides* (PA) tissue from four Southeast Florida reefs.

(A) Principal coordinate analysis (PCoA) with a weighted UniFrac distance, colored by coral host-species, labeled by the month of collections and shapes are based on reef location. (B) Constrained correspondence analysis (CCA) with a Bray-Curtis statistic for microbial compositional dissimilarity. The microbiome correspondence analysis was constrained by temperature [°C], alongshore currents [m s^{-1}], significant wave height [m], and relative turbidity (normalized). Each sample is colored by month of collection, and shapes are based on reef location.

[Figure: PCoA and CCA plots]
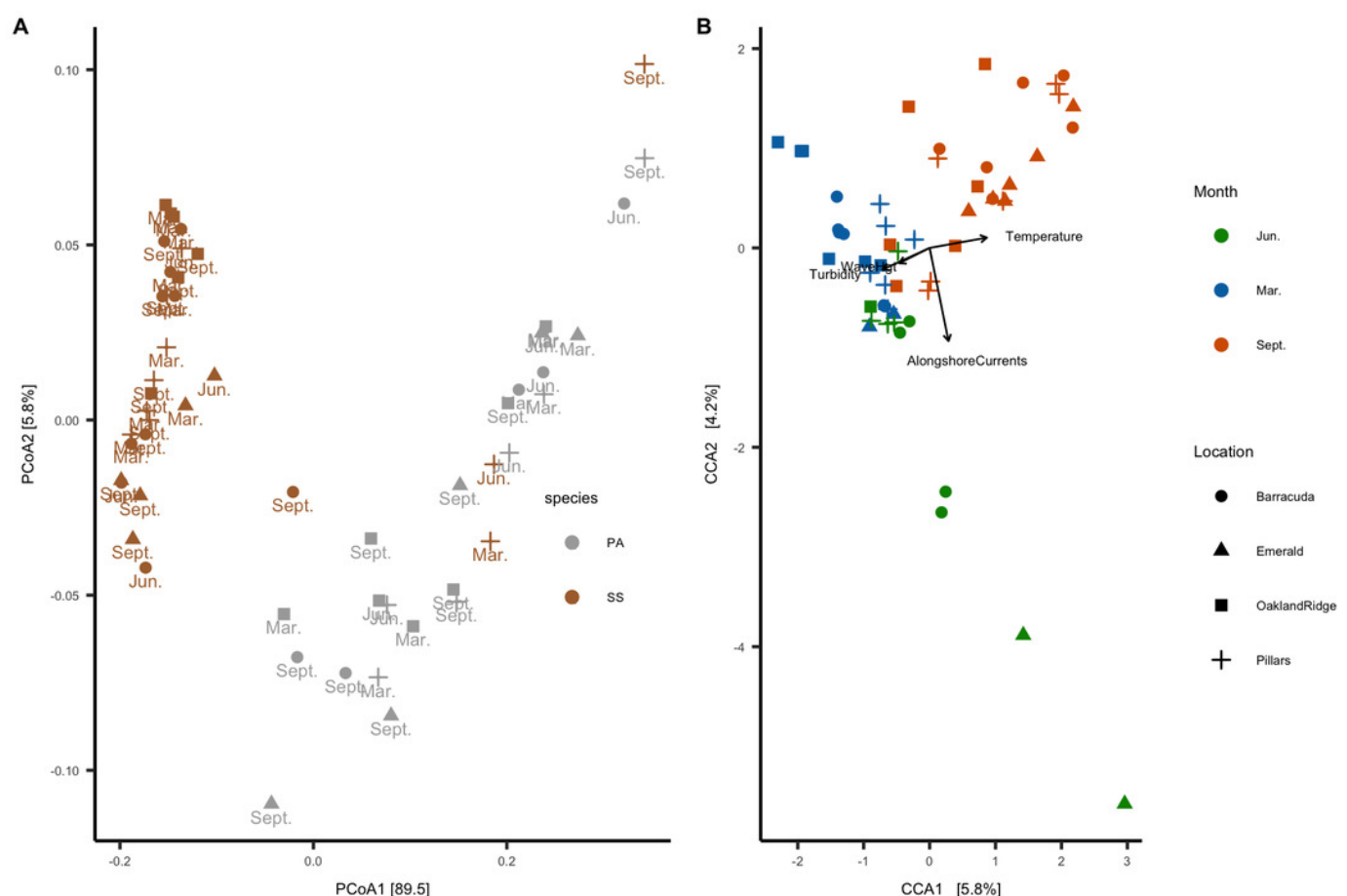
Figure 7

Microbial taxa that correlated with physical habitat variables in Southeast Florida reefs.

Samples are colored by microbial order. The colored line represents the linear regression fit between the habitat variable (x axis) and the microbe's relative abundance (y axis); grey shadow around the line is the 95% confidence interval. Plots show microbial taxa vs. physical habitat variables that were found to be significantly correlated to ($p < 0.05$, $R^2 > 0.2$) (A) significant wave height [m] and (B) temperature [°C].